Journal of Food Measurement and Characterization (2025) 19:8899–8908
https://doi.org/10.1007/s11694-025-03564-4

ORIGINAL PAPER

Determination of quality levels of fish oils recovered from trout waste using machine learning and odor sensors

Emre Yavuzer[1] · Dilek Yaprak Uslu[2] · Memduh Köse[3] · Mehmet Yetişen[1] · Hamza Alaşalvar[1] · Halil İbrahim Şimşek[1]

Received: 23 April 2025 / Accepted: 5 August 2025 / Published online: 5 September 2025
© The Author(s), under exclusive licence to Springer Science+Business Media, LLC, part of Springer Nature 2025

Abstract

In this study, chemical analyses and low-cost gas sensor measurements were conducted to determine the oxidative stability of fish oils obtained through enzymatic hydrolysis from rainbow trout (*Oncorhynchus mykiss*) waste. The initial EPA and DHA contents of the extracted oils were 1.31% and 4.94%, respectively, with oleic acid (C18:1n9) being the most abundant fatty acid at 38.59%. During a 20-day storage period, changes in free fatty acids, peroxide value, conjugated dienes, conjugated trienes, *p*-anisidine, and thiobarbituric acid values were monitored, along with alterations in fatty acid composition. Additionally, odor intensity was assessed using an electronic nose system. Sensor responses exhibited significant variations at different stages of the oxidative process, with MQ131 and MQ138 sensors demonstrating sensitivity to primary oxidation, while MQ3 and MQ135 sensors provided strong signals associated with the increase in secondary oxidation products. Overall, the study demonstrates the feasibility of using low-cost gas sensors for real-time oxidation assessment, contributing to improved fish oil stability management.

Keywords Trout waste · Fish oil · Enzymatic hydrolysis · Oxidative stability · Electronic nose · Gas sensors · Lipid oxidation · Machine learning

Introduction

Commercial trout production has grown substantially in the last decade due to its favorable sensory characteristics, ease of cultivation, and suitability for processing [1]. Fish, in general, are recognized as excellent sources of high-quality protein, healthy fats, omega-3 fatty acids, vitamins, and minerals—making them nutritionally superior to many other food sources [2].

Crude fish oil, typically extracted from marine and freshwater fish by-products, has gained wide attention for its functional lipid profile [3]. It is increasingly used in food, cosmetics, pharmaceuticals, and biofuel industries [4–6]. Apart from its direct consumption after pharmaceutical refinement, crude fish oil is valuable in aquaculture feed, biodiesel production, and other biotechnological applications [4, 7, 8].

The health benefits of fish oil are mainly attributed to its high levels of eicosapentaenoic acid (EPA; 20:5n-3) and docosahexaenoic acid (DHA; 22:6n-3), which are long-chain n-3 polyunsaturated fatty acids (PUFAs). These compounds play essential roles in cardiovascular health, brain development, and inflammation regulation [9–13]. DHA in particular, is a major structural component of the brain, heart, and retina [10], while EPA has been shown to support the treatment of neurological diseases and some cancer [14]. Children and the elderly have a greater physiological demand for these fatty acids [15], and their deficiency has been linked to inflammatory markers and cognitive disorders such as Alzheimer's disease [16].

✉ Mehmet Yetişen
mehmetyetisen@ohu.edu.tr

1 Department of Food Engineering, Faculty of Engineering, Niğde Ömer Halisdemir University, Niğde 51240, Türkiye

2 Department of Cookery, Vocational School of Social Sciences, Niğde Ömer Halisdemir University, Niğde 51240, Türkiye

3 Department of Electrical Electronics Engineering, Faculty of Engineering and Architecture, Kırşehir Ahi Evran University, Kırşehir 40100, Türkiye

As a functional food provides significant health benefits when consumed fresh, with its nutritional integrity preserved [17]. Rising global population and growing awareness of healthy eating habits have further highlighted the nutritional and functional value of species such as trout. Despite its advantages, fish oil is highly susceptible to oxidative degradation, which negatively affects its odor, color, and shelf life [18, 19]. Traditional quality evaluation methods rely on trained sensory panelists, but human perception is subjective and may introduce variability [1]. Recently, electronic nose (e-nose) systems have emerged as promising tools for objective and real-time assessment of odor profiles [20–27]. These systems, often built on open-source platforms like Arduino, are cost-effective, scalable, and suitable for industrial integration. They offer advantages such as real-time data acquisition, sensor automation, and ease of customization.

For oil extraction, enzymatic hydrolysis presents a safe and sustainable alternative to solvent-based or mechanical methods [28]. It operates under mild conditions, avoids harmful residues, and enables simultaneous recovery of valuable proteins. When optimized, enzymatic extraction yields high-quality oil from viscera and lipid-rich tissues, making it ideal for valorizing fish processing waste.

Therefore, the aim of this study is to evaluate the oxidative stability of fish oils extracted from rainbow trout (*Oncorhynchus mykiss*) waste using enzymatic hydrolysis. This evaluation integrates chemical oxidation indicators, sensor-based odor analysis, and deep learning algorithms for quality prediction. The study also aims to explore correlations between classical indicators (e.g., PV, TBA) and sensor responses, demonstrating the potential of low-cost e-nose systems in real-time quality monitoring. The findings are expected to contribute to more sustainable oil processing and smart storage monitoring solutions for the fish industry.

Materials and methods

Electronics components used in device

In this study, the data input and output of odor sensors were processed using the open-source physical programming platform Arduino Mega 2560 R3. The Arduino Mega 2560 R3 development board is a microcontroller board based on the ATmega 2560, featuring 54 digital input/output pins. Due to the necessity of using multiple sensors, the Arduino Mega Sensor Shield was also employed. The electronic nose system previously developed in our study [24] was modified and enhanced with additional sensors to improve its performance.

The newly developed electronic nose system used in this study was built using the Arduino Mega 2560 R3 microcontroller and an Arduino Mega Sensor Shield to accommodate multiple sensor inputs. The sensor array consisted of 12 metal oxide semiconductor (MOS) gas sensors, each selected for its relevance to volatile compounds produced during fish oil oxidation. These sensors operate based on the principle of changes in electrical resistance in the presence of specific gases. MQ3: Sensitive to alcohols and organic solvents. Alcohols such as ethanol and aldehydes are common secondary oxidation products of lipids. MQ4: Detects methane, a minor by-product of anaerobic microbial activity, potentially relevant in late spoilage stages. MQ5: Responds to various hydrocarbons, which are generated during oxidative decomposition of unsaturated fatty acids. MQ9: Sensitive to carbon monoxide and methane. CO may indicate thermal degradation or microbial spoilage processes. MQ131: Detects ozone and nitrogen oxides, which may not be direct by-products but can be present due to environmental contamination or advanced oxidation stages. MQ135: Highly sensitive to ammonia, sulfide, and benzene — key indicators of protein breakdown and oxidative rancidity. MQ136: Targets sulfur compounds such as hydrogen sulfide, often released during the degradation of sulfur-containing amino acids. MQ137: Specifically designed for ammonia detection, correlating with spoilage and degradation of amino acids. MQ138: Detects a wide range of volatile organic compounds (VOCs) and alcohols, making it useful for capturing overall odor profile changes. MQ139: Another VOC-sensitive sensor that complements MQ138 by broadening the spectrum of detectable organic compounds. MG811: Measures CO_2 concentration, which can rise due to microbial respiration and general spoilage progression. TGS813: Detects methane and butane, which may be minor indicators of advanced spoilage.

Prior to data collection, the device was operated for 30 min without a sample to establish a baseline for background odors. Subsequently, 2.0 mL of fish oil was placed in a 20 mL sealed glass vial with a gas-tight septum, and the headspace was allowed to equilibrate for 10 min at room temperature. The sensor array was then exposed to the sample headspace. Sensor responses were recorded continuously over a 2-minute period. For each measurement, the peak sensor signal was extracted and normalized relative to baseline values obtained from clean air. The ambient conditions in the measurement chamber were maintained at 23 ± 1 °C and 45–55% relative humidity. Sensor responses were recorded continuously over a 2-minute period. For each measurement, the peak sensor signal was extracted and normalized relative to baseline values obtained from clean air prior to sample exposure. The operating temperature and humidity in the measurement chamber were maintained at

ambient conditions (23 ± 1 °C, 45–55% RH). Furthermore, electronic nose box construction with sensors was shown in Fig. 1.

The system consists of a custom-fabricated plastic chamber with a total volume of approximately 2.5 L, designed to accommodate the sensor array and sample vials. The chamber includes a sealed inlet for filtered ambient air and a dedicated outlet for controlled ventilation, allowing for repeatable headspace analysis without cross-contamination. Compared to commercial electronic nose platforms, the system developed in this study offers several advantages. First, it is low-cost and open-source, utilizing readily available components, such as MQ-series sensors and Arduino hardware. Second, the modular design allows for easy replacement or addition of sensors, providing flexibility for different sample types. Third, the system is compact and portable, making it suitable for on-site quality control in food processing environments. While commercial systems often require complex software and high initial investment, this system provides reliable discrimination capability with minimal resources, making it an attractive option for small- to medium-scale industries and research laboratories.

Deep learning

In this study, ResNet, a widely used class of deep neural networks for image classification, was employed. Images of fish oil samples were captured using a high-resolution smartphone camera (12 MP) under controlled lighting conditions. Each image was taken against a white background to minimize environmental noise and maintain consistency. The dataset comprised a total of 1000 images. All images were resized to 224 × 224 pixels to match the input dimensions required by the ResNet architectures. Prior to model input, standard image normalization techniques were applied (mean subtraction and scaling to [0,1]). ResNet-50 is a deep learning model with 50 layers, pre-trained on the ImageNet database, which contains over one million images categorized into 1,000 classes. What makes ResNet particularly effective for image recognition is its deep architecture, comprising more than 23 million trainable parameters. Utilizing a pre-trained model is one of the effective approaches for classification. While other pre-trained deep models, such as AlexNet and GoogleNet are available, ResNet-50 stands out due to its lower error rate and superior generalization performance in recognition and classification tasks.

In the classification of oil images, feature extraction was performed using the pre-trained ResNet-18 and ResNet-50 models, followed by classification using support vector machines (SVMs).

Fish oil production and storage conditions

Rainbow trout (*Oncorhynchus mykiss*) waste was obtained from a local fishmonger in Niğde. The collected fish waste was transported to the laboratory under a cold chain and stored at −20 °C until the experiments commenced. To extract fish oil from trout waste, the samples were minced using a meat grinder and mixed with distilled water at a 1:1 ratio. The mixture was then placed in a shaking water bath set to 60 °C, with continuous temperature monitoring until the homogenate reached 55 °C. Once stabilized at this temperature, the pH was adjusted to 8 using 1 N sodium hydroxide (NaOH). Enzymatic hydrolysis was initiated by adding 0.5% (w/w) Alcalase® 2.4 L FG (Novozymes A/S, Bagsværd, Denmark), a serine endopeptidase derived from *Bacillus licheniformis*, with a declared activity of 2.4 AU/g (Anson units per gram). The enzyme dosage corresponded to 5 mL per kg of wet fish tissue, and the hydrolysis was carried out for 60 min at 55 °C with continuous shaking at 150 rpm to ensure uniform mixing and optimal enzyme activity. After the reaction, the hydrolysate was cooled to

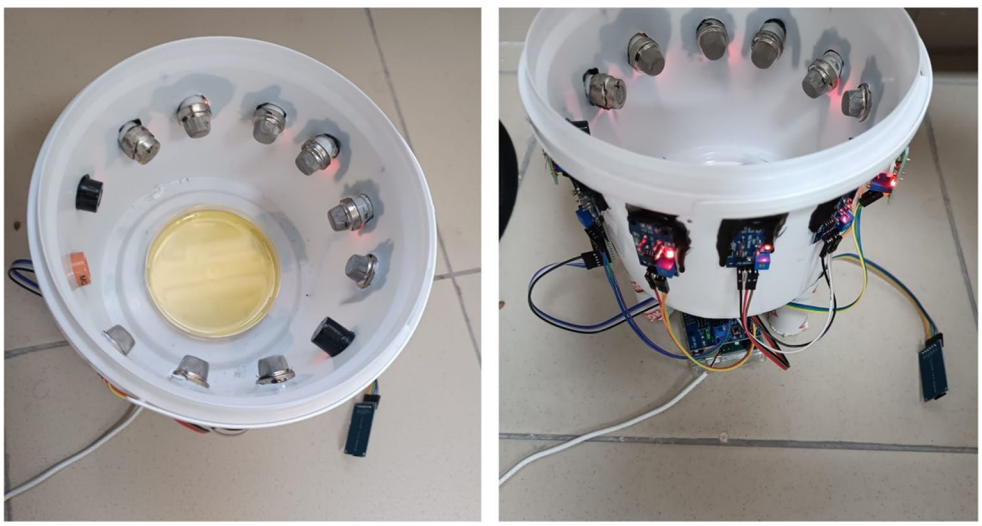

Fig. 1 Electronic nose box construction with MQ3, MQ4, MQ5, MQ9, MQ131, MQ135, MQ136, MQ137, MQ138, MQ139, MG811 and TGS813 sensors

room temperature, filtered through a double-layer cheesecloth, and centrifuged at 5,000 × g for 20 min at 4 °C. The upper lipid layer was carefully collected and stored in dark, tightly sealed glass bottles at 4 °C until analysis.

Peroxide value (PV)

PV was determined and expressed as milliequivalents (meq) of peroxide oxygen per kilogram of oil. Briefly, 2 g of fish oil was dissolved in a mixture of acetic acid and chloroform. Potassium iodide (KI) was added, and the liberated iodine was titrated with 0.01 N sodium thiosulfate solution using starch as an indicator. The peroxide value was calculated and expressed as milliequivalents of active oxygen per kilogram of oil (meq O_2/kg) [29].

Free fatty acid (FFA) analysis

The FFA content was analyzed following method [30]. A 5 g sample of the extracted trout oil was placed in a 250 mL Erlenmeyer flask. A 50–100 mL mixture of diethyl ether and ethanol (25:25 mL) was added, and the solution was shaken for 2 min to dissolve the oil and fatty acids. Subsequently, 1 mL of 1% phenolphthalein indicator was added, and the mixture was titrated with 0.1 N sodium hydroxide until a persistent pink color was observed for at least 15 s. The percentage of free fatty acids (expressed as oleic acid) was then calculated using the formulas provided below.

$$FFA\ (\%\ Oleic\ acid) = \frac{(A - B) \times\ 2.805}{g} \quad (1)$$

A: Consumed volume for sample 0,1 N NaOH quantity (ml).
B: Amount of 0.1 N NaOH spent for the blank (ml).
m: Sample quantity (g).
2.805: Conversion factor.

Thiobarbituric acid (TBA) analysis

The TBA analysis was conducted according to the method [31]. 0.5 g oil sample was weighed into a 25 mL volumetric flask, and a small amount of 1-butanol was added. The flask was gently shaken to dissolve the oil in butanol, and the solution was brought to a final volume of 25 mL with butanol. A 5 mL aliquot of this solution was transferred into a test tube, and 5 mL of freshly prepared 2-TBA reagent was added. The test tube was sealed and incubated in a boiling water bath for 2 h. After cooling to room temperature, the absorbance of the colored complex was measured at 532 nm using a UV spectrophotometer. The malondialdehyde (MDA) content was calculated using the following formula.

$$\mathrm{A} = \varepsilon \times \mathrm{b} \times \mathrm{c} \quad (2)$$

Ɛ: Molar absorbance coefficient for MAD-TBA.
b: Light path length.
c: Concentration.
p-anisidine value.

The *p*-anisidine analysis was performed according to the method described by [32]. A 0.5 g sample of oil extracted from trout waste was weighed into a 25 mL Falcon tube, followed by the addition of 10 mL of isooctane. The mixture was thoroughly homogenized, and a 2.5 mL aliquot of the resulting solution was transferred into a separate container. Subsequently, 0.5 mL of p-anisidine reagent was added, and the mixture was allowed to react for 10 min. A blank solution was prepared by mixing 2.5 mL of isooctane with 0.5 mL of p-anisidine reagent and incubating for the same duration. The absorbance of the samples was measured at 350 nm.

Fatty acid profile

Fatty acid methyl esters (FAMEs) were prepared from the extracted lipid following the method [33]. A 25 mg sample of the extracted oil was mixed with 4 mL of 2 M KOH and 2 mL of n-heptane. The mixture was vortexed at room temperature for 2 min and then centrifuged at 4000 rpm for 10 min. The upper heptane phase was collected for gas chromatography (GC) analysis.

Statistical analysis

Analyses were run in triplicate and results were reported as mean values ± standard deviation (S.D). The results were analyzed with variance analysis (ANOVA) and Tukey's multiple range test using Mintab 18.1 (Minitab, Inc., USA) software. Pearson correlation analysis was conducted using OriginPro 2021 software (OriginLab Corporation, MA, USA). Levels for significant differences were set at $p < 0.05$.

Results and discussion

In this study, the quality levels of fish oils obtained from trout waste through enzymatic hydrolysis were assessed using chemical, sensory, and gas sensor data throughout the storage period.

The fatty acid composition (%) of the oils obtained from waste products is presented in Table 1. When evaluating the fatty acid composition, no significant changes were observed in the levels of saturated fatty acids (SFA) during storage. However, minor but statistically significant differences ($p < 0.05$) were detected in the levels of

Table 1 Fatty acid contents of fish oils obtained by enzymatic hydrolysis from trout waste (%)

	0	1	4	6	11	15	20
C12:0	0.03 ± 0.00^{a}	0.03 ± 0.00^{a}	0.03 ± 0.00^{a}	0.03 ± 0.00^{ab}	0.03 ± 0.00^{a}	0.03 ± 0.00^{a}	0.03 ± 0.00^{a}
C14:0	1.90 ± 0.01^{a}	1.92 ± 0.00^{a}	1.93 ± 0.00^{a}	1.92 ± 0.00^{a}	1.92 ± 0.00^{a}	1.92 ± 0.00^{a}	1.92 ± 0.00^{a}
C15:0	0.19 ± 0.00^{a}	0.19 ± 0.00^{a}	0.19 ± 0.00^{a}	0.19 ± 0.00^{a}	0.19 ± 0.00^{a}	0.19 ± 0.00^{a}	0.19 ± 0.00^{a}
C16:0	12.82 ± 0.12^{a}	12.71 ± 0.01^{a}	12.73 ± 0.00^{a}	12.71 ± 0.02^{a}	12.70 ± 0.00^{a}	12.71 ± 0.00^{a}	12.70 ± 0.00^{a}
C17:0	0.56 ± 0.00^{a}	0.56 ± 0.00^{a}	0.56 ± 0.00^{a}	0.56 ± 0.00^{a}	0.56 ± 0.00^{a}	0.56 ± 0.00^{a}	0.56 ± 0.00^{a}
C18:0	3.55 ± 0.00^{a}	3.55 ± 0.00^{a}	3.55 ± 0.00^{a}	3.56 ± 0.01^{a}	3.55 ± 0.00^{a}	3.55 ± 0.00^{a}	3.55 ± 0.00^{a}
C22:0	1.36 ± 0.00^{a}	1.36 ± 0.00^{a}	1.34 ± 0.00^{a}	1.35 ± 0.00^{a}	1.35 ± 0.00^{a}	1.34 ± 0.01^{a}	1.35 ± 0.00^{a}
∑SFA*	20.41	20.32	20.37	20.34	20.35	20.35	20.35
C15:1	0.02 ± 0.00^{a}	0.02 ± 0.00^{a}	0.02 ± 0.00^{a}	0.02 ± 0.00^{a}	0.02 ± 0.00^{a}	0.02 ± 0.00^{a}	0.02 ± 0.00^{a}
C16:1	3.87 ± 0.01^{a}	3.87 ± 0.00^{a}	3.89 ± 0.00^{a}	3.88 ± 0.00^{a}	3.88 ± 0.00^{a}	3.88 ± 0.00^{a}	3.87 ± 0.00^{a}
C17:1	0.27 ± 0.00^{a}	0.27 ± 0.00^{a}	0.27 ± 0.00^{a}	0.27 ± 0.00^{a}	0.27 ± 0.00^{a}	0.27 ± 0.00^{a}	0.27 ± 0.00^{a}
C18:1n9	38.59 ± 0.03^{a}	38.68 ± 0.01^{ab}	38.83 ± 0.00^{b}	38.80 ± 0.05^{bc}	38.91 ± 0.01^{c}	38.86 ± 0.01^{c}	38.83 ± 0.02^{c}
C22:1n9	0.48 ± 0.00^{a}	0.48 ± 0.00^{a}	0.46 ± 0.00^{a}	0.47 ± 0.01^{a}	0.46 ± 0.01^{a}	0.46 ± 0.00^{a}	0.46 ± 0.00^{a}
C24:1n9	0.88 ± 0.01^{a}	0.87 ± 0.01^{a}	0.85 ± 0.00^{a}	0.83 ± 0.08^{a}	0.88 ± 0.01^{a}	0.87 ± 0.01^{a}	0.86 ± 0.00^{a}
∑MUFA**	44.11	44.19	44.32	44.27	44.42	44.36	44.31
C18:2n6	19.74 ± 0.02^{a}	19.79 ± 0.00^{ab}	19.86 ± 0.00^{b}	19.82 ± 0.03^{b}	19.85 ± 0.00^{b}	19.82 ± 0.01^{b}	19.81 ± 0.00^{ab}
C18:3n6	0.61 ± 0.00^{a}	0.61 ± 0.00^{a}	0.59 ± 0.00^{a}	0.59 ± 0.02^{a}	0.60 ± 0.00^{a}	0.60 ± 0.00^{a}	0.59 ± 0.00^{a}
C18:3n3	4.03 ± 0.03^{a}	4.03 ± 0.00^{a}	4.03 ± 0.00^{a}	4.01 ± 0.03^{a}	4.03 ± 0.00^{a}	4.02 ± 0.00^{a}	4.03 ± 0.02^{a}
C20:2 cis	2.50 ± 0.01^{a}	2.51 ± 0.00a	2.51 ± 0.00^{a}	2.51 ± 0.01^{a}	2.52 ± 0.00^{a}	2.52 ± 0.01^{a}	2.51 ± 0.00^{a}
C20:3 n6	0.67 ± 0.00^{a}	0.68 ± 0.01^{a}	0.68 ± 0.00^{a}	0.67 ± 0.01^{a}	0.68 ± 0.00^{a}	0.68 ± 0.00^{a}	0.68 ± 0.01^{a}
C20:4 n6	0.54 ± 0.01^{a}	0.54 ± 0.00^{a}	0.53 ± 0.00^{a}	0.54 ± 0.00^{a}	0.54 ± 0.00^{a}	0.53 ± 0.00^{a}	0.53 ± 0.00^{a}
C20:5n3	1.31 ± 0.01^{c}	1.29 ± 0.01^{bc}	1.28 ± 0.00^{bc}	1.30 ± 0.01^{bc}	1.25 ± 0.00^{a}	1.28 ± 0.00^{ab}	1.25 ± 0.00^{a}
C22:6 n3	4.94 ± 0.04^{c}	4.91 ± 0.01^{bc}	4.73 ± 0.01^{a}	4.83 ± 0.00^{b}	4.67 ± 0.00^{a}	4.74 ± 0.01^{a}	4.68 ± 0.00^{a}
∑PUFA***	34.34	34.36	34.21	34.27	34.14	34.19	34.08
PUFA/SFA	1.68	1.69	1.68	1.68	1.68	1.68	1.67
∑ ω3	10.28	10.23	10.04	10.14	9.95	10.04	9.96
∑ ω6	21.56	21.62	21.66	21.62	21.67	21.63	21.61
∑ ω6/∑ ω3	2.10	2.11	2.16	2.13	2.18	2.15	2.17
EPA	1.31	1.29	1.28	1.30	1.25	1.28	1.25
DHA	4.94	4.91	4.73	4.83	4.67	4.74	4.68
DHA/EPA	3.77	3.81	3.70	3.72	3.74	3.70	3.74

**SFA*, Saturated fatty acid, ***MUFA*, Monounsaturated fatty acid, ****PUFA*, Polyunsaturated fatty acid. Different letters (a − d) in the same fraction show significant differences ($p < 0.05$)

monounsaturated fatty acids (MUFA) and polyunsaturated fatty acids (PUFA). In particular, the observed decrease in PUFA levels over time is thought to be a result of oxidative deterioration. The declining levels of EPA (C20:5n3) and DHA (C22:6n3) further support the susceptibility of omega-3-rich fish oils to oxidation during long-term storage. The changes observed in the DHA/EPA ratio suggest that oxidative degradation affects specific long-chain fatty acids at different rates. Pearson correlation analysis was also performed to further investigate the relationship between changes in fatty acids and quality parameters. Peroxide, p-anisidine, and TBA values displayed a strong negative correlation with EPA and DHA values. The correlation coefficients (r) for PV-EPA and PV-DHA were −0.95 and −0.99, respectively. Moreover, *p*-ansidine values were negatively correlated with EPA ($r = -0.77$) and DHA ($r = -0.86$). Additionally, a strong negative correlation existed between TBA-EPA ($r = -0.92$) and TBA-DHA ($r = -0.97$). These findings revealed that an increase in oxidation indicators corresponded to a decrease in EPA and DHA. The relationship between TBA and oxidation of EPA/DHA was also reported by Chu et al. [34].

These results are in agreement with previous studies. For example, Golmakani et al. [35] reported that fish oils obtained from rainbow trout waste using microwave-assisted transesterification contained 45.9% PUFA and 33.15% MUFA, which are in the same range as the initial composition in our study. However, our study observed a clearer decline in PUFA content during storage, likely due to the enzymatically hydrolyzed matrix being more prone to oxidative degradation due to the presence of hydrolyzed proteins or free radicals. Fiori et al. [36], using supercritical CO_2 extraction and the Randall method, found PUFA contents ranging from 72.6 to 75.7% depending on tissue type. While those values were slightly higher than our results, it is worth noting that supercritical CO_2 offers strong oxidative protection due to its oxygen-free environment. In contrast, our enzymatic method operates under ambient oxygen and

may permit more oxidation during extraction and early storage stages. These differences highlight the role of extraction method and processing atmosphere in determining oxidative behavior and fatty acid stability.

The obtained results provide significant insights into the oxidative stability of fish oils. Table 2 presents the values of free fatty acids (FFA, %), PV (meq O_2/kg), K232 (conjugated dienes, Abs/g), K270 (conjugated trienes, Abs/g), *p*-anisidine, and TBA. FFA content is a key indicator of enzymatic lipolysis [37]. Throughout the storage period, notable fluctuations in FFA percentages were observed, with an increase detected on day 20 compared to the initial level. However, this increase was not statistically significant ($p > 0.05$). This finding suggests that the release of fatty acids due to lipases and other hydrolytic enzymes present in the oil after enzymatic hydrolysis continued during storage, indicating ongoing lipolytic activity.

In another study, the FFA levels of fish oils obtained from trout waste at different temperatures remained unchanged throughout the storage period. However, oils produced at 90 °C exhibited higher FFA levels, which influenced oxidative stability, as FFA is known to promote oxidation [38, 39].

Ambient temperature in the storage environment was regularly monitored using a calibrated digital thermometer, and no significant temperature fluctuations were observed during the experimental period. The sharp increase in PV after day 11 likely reflects the exponential phase of hydroperoxide formation, a hallmark of primary lipid oxidation. This lag phase, followed by a steep rise suggests that the antioxidant potential of endogenous compounds was exhausted, allowing autooxidation to proceed rapidly. Interestingly, this inflection point in PV coincides with the increased sensitivity of MQ131, a sensor known to detect ozone and NOx-type oxidants, suggesting a possible link between hydroperoxide breakdown and oxidative VOC release. Although a slight decrease was observed on day 20, these values indicate the onset of significant oxidative deterioration in the oil. However, the slight decrease observed in PV on day 20 warrants further discussion. Several factors may contribute to this decline. Firstly, hydroperoxides are not stable end products and may undergo decomposition into secondary oxidation products such as aldehydes, ketones, and alcohols, especially under ambient storage conditions [40]. This breakdown reduces measurable PV despite ongoing oxidation. Secondly, experimental conditions such as temperature fluctuations, oxygen availability, or sample handling may have influenced peroxide decomposition or evaporation of volatile intermediates. These combined factors likely contributed to the observed PV reduction, which does not necessarily indicate an improvement in oil quality but rather a progression in the oxidation pathway. A study on fish oils obtained from trout waste reported initial PV ranging from 0.82 to 4.13 meq O_2/kg, which increased to approximately 15 meq O_2/kg after 91 days of storage at 20 °C. In oils produced at 90 °C, peroxide levels were consistently higher than those of conventional oils, whereas no significant differences were observed in oils produced at 70 °C [38]. Furthermore, a study on ultrasound-assisted fish oil extraction and purification using adsorbents from rainbow trout intestines reported a PV of 29 meq O_2/kg. The FFA content was also determined as 1.41% in terms of oleic acid [41].

The conjugated diene (CD) value is a crucial parameter for assessing the extent and effectiveness of lipid degradation [42]. Both CD and conjugated triene (CT) values exhibited similar trends as indicators of oxidative deterioration, reaching their maximum levels on day 11. However, after day 15, a significant decrease in CD levels was observed, likely due to the formation of secondary oxidation products.

The oxidative stability of lipids obtained from trout waste (muscle and internal organs) under accelerated oxidation conditions was assessed over a 10-day storage period by monitoring primary and secondary oxidation products. CD values, representing primary oxidation products, showed an increasing trend in both muscle and organ lipids throughout storage [43]. In another study, fish oil extracted via enzymatic hydrolysis from high-pressure (HP) pre-treated rainbow trout and Atlantic salmon raw material exhibited a significant increase in CD values over a 4-week storage period. Similarly, CT values also increased with prolonged storage [40].

The measurement of secondary lipid oxidation products serves as a reliable quality parameter for evaluating chemical changes induced by various processing applications [44]. Among these indicators, the *p*-anisidine value showed a

Table 2 Quality parameters of oil obtained from waste of trout during storage

	0	1	4	6	11	15	20
Free fatty acids (%)	0.46 ± 0.03^{a}	0.47 ± 0.03^{a}	0.45 ± 0.05^{a}	0.49 ± 0.03^{a}	0.47 ± 0.02^{a}	0.43 ± 0.02^{a}	0.52 ± 0.15^{a}
Peroxide value (meq O_2/kg)	1.96 ± 0.39^{c}	2.51 ± 0.16^{c}	4.01 ± 0.69^{bc}	5.77 ± 0.19^{b}	17.74 ± 0.97^{a}	18.64 ± 1.22^{a}	17.24 ± 2.07^{a}
K_{232} (Abs/g)	44.93 ± 4.32^{bc}	55.05 ± 3.64^{ab}	31.55 ± 2.42^{bc}	39.07 ± 1.35^{bc}	79.92 ± 27^{a}	14.68 ± 1.28^{c}	39.63 ± 7.8^{bc}
K_{270} (Abs/g)	4.13 ± 0.16^{ab}	4.68 ± 0.14^{a}	2.59 ± 0.29^{c}	3.35 ± 0.19^{abc}	4.22 ± 1.09^{ab}	0.98 ± 0.24^{d}	2.99 ± 0.84^{bc}
p-anisidine	7.76 ± 0.28^{c}	10.42 ± 0.17^{b}	10.13 ± 0.72^{b}	10.49 ± 0.13^{b}	10.55 ± 0.21^{b}	13.36 ± 0.05^{a}	11.00 ± 0.23^{b}
Thiobarbituric acid	2.49 ± 0.19^{d}	3.16 ± 0.1^{d}	3.21 ± 0.21^{d}	7.76 ± 0.37^{c}	14.76 ± 0.74^{b}	21.05 ± 0.78^{a}	22.22 ± 0.45^{a}

Different letters (a − d) in the same line show significant differences ($p < 0.05$)

continuous increase during storage, peaking at 13.36 ± 0.05 on day 15. A similar trend was observed in fish oils derived from trout waste at different processing temperatures, where the *p*-anisidine value increased with extended storage duration [38]. Previous work reported that salt treatment significantly reduced lipase activity in rainbow trout viscera. This reduction in lipase activity led to a decrease in lipolysis and FFA formation, subsequently slowing down oxidation and resulting in lower peroxide and *p*-anisidine values [45, 46].

The significant increase in TBA values throughout the storage period suggests an active progression of secondary lipid oxidation, resulting in the accumulation of malondialdehyde (MDA). This outcome is expected, given the high PUFA content of trout oil, particularly EPA and DHA, which are highly susceptible to oxidative cleavage. The consistent rise in TBA coincided with intensified sensor responses (especially MQ138), supporting the hypothesis that sensors were detecting aldehydic volatiles derived from MDA breakdown products. Therefore, sensor signals may serve as a real-time proxy for non-volatile secondary oxidation indicators. These findings suggest that lipid oxidation progressed throughout storage, leading to a substantial decline in sensory quality. The average TBA values exceeded the recommended threshold for fish products (3 mg/kg) [47]. A study investigating the quality parameters of oil obtained from trout waste after being held at room temperature for specific periods before freezing at −28 °C reported that TBA values ranged from 0.11 to 0.19 mg malondialdehyde/kg oil. Notably, an increase in the holding time before freezing was associated with a significant rise in TBA values [48]. Similarly, increasing TBA values during storage were also reported in oils extracted from Caspian whitefish (*Rutilus frisii kutum*) and Nile perch (*Lates niloticus*) when the freezing process was delayed. This trend highlights the impact of pre-freezing holding time on lipid oxidative stability [49].

The potential of Arduino-based gas sensors to rapidly detect oxidative deterioration has been explored. To ensure data accuracy, the sensors were calibrated using the Arduino Mega 2560 R3. Before each measurement, the system was stabilized in clean air for 30 min, and baseline signals (V_o) were recorded. Sensor responses were calculated by subtracting these baselines from the sample readings ($\Delta V = Vsample - V_o$). All signals were normalized (0–1 scale) to reduce sensor-to-sensor variation. Calibration and data collection were programmed via the Arduino using custom code. As shown in Table 3, specifically, MQ3, MQ131, MQ135, and MQ138 sensors demonstrated significant sensitivity in detecting oxidation-related odor increases in fish oils compared to other sensors. Notably, their responses correlated strongly with key indicators of oxidative stability, such as PV and TBA value.

Table 3 Daily odor changes in fish oil during storage

Days	MQ3	MQ4	MQ5	MQ9	MQ131	MQ135	MQ136	MQ137	MQ138	MQ139	MG811	TGS813
0	−14.46	−21.69	−10.92	−18.54	−5.31	−2.08	−17.62	19.46	−16.92	−14.00	−0.38	−25.31
1	15.04	−35.24	−8.52	7.4	4.68	−8.16	16.16	−33.12	18.36	18.6	−39.4	12.2
4	24.73	−37.62	−30.27	−23.32	7.62	45.06	12.27	19.60	39.86	21.86	−8.51	10.40
6	14.83	0.13	0.96	−18.71	0.92	−0.29	12.54	7.21	5.50	3.08	0.63	−3.42
11	16.50	12.88	3.25	21.67	25.50	20.29	26.50	−33.00	18.63	−4.00	8.00	26.75
15	18.79	−19.18	−9.20	−21.92	6.58	31.17	53.57	25.74	54.00	30.32	−0.40	15.50
20	25.81	−30.00	−20.65	−9.20	97.50	35.15	155.15	34.57	41.07	25.75	0.38	4.33

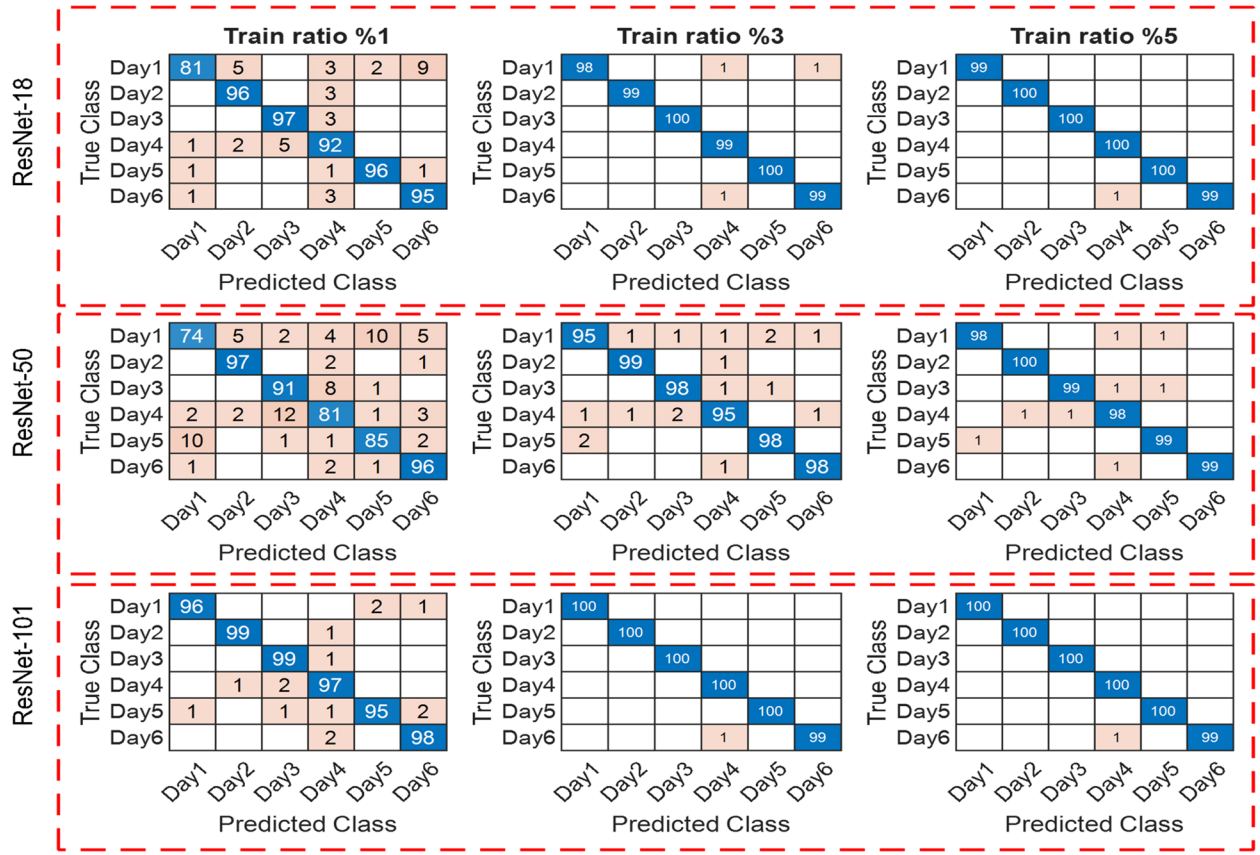

Fig. 2 Classification performance error matrix (confusion matrix) for ResNet-101, ResNet18 and ResNet50 models with training rate 1%, 3%, 5%

Among these, MQ131 and MQ138 exhibited increasing signal intensities over time, indicating the production of oxygenated volatile compounds (e.g., aldehydes, ketones, and alcohols) as oxidation progressed. The response of MQ131 reached 97.50 units on day 20 (from an initial value of −5.31), reflecting the breakdown of hydroperoxides into secondary oxidation products, even though PV levels remained relatively stable after day 15. Similarly, MQ138 displayed a response pattern parallel to PV, with a significant increase on days 15 and 20. Given its sensitivity to organic solvents and oxidation-derived volatile compounds, MQ138 effectively detected the presence of secondary oxidation products, such as hexanal, pentanal, and malondialdehyde, resulting from hydroperoxide decomposition. Additionally, MQ3 (sensitive to alcohols) showed a moderate but consistent rise, suggesting progressive lipid degradation. These results reinforce the applicability of sensor data as real-time indicators of oxidative quality. The observed trends also show a strong correlation with chemical parameters discussed in Table 2, further validating the predictive value of the electronic nose system in monitoring fish oil stability.

In the classification of oil images, features were extracted using pretrained ResNet-18 and ResNet-50 models, followed by classification with support vector machines. The classification performance confusion matrix for training ratios of 1%, 3%, and 5% are presented in Fig. 2. The results indicate that as the training ratio increased, classification accuracy improved significantly. Each class contained 1,000 samples, meaning that at a 3% training ratio, 30 samples were used for training while 970 were allocated for testing. When features were extracted and classified using the ResNet-18 model, a classification accuracy of 99% was achieved, whereas the ResNet-50 model yielded an accuracy of 97.2%. When the training ratio exceeded 20%, both models approached nearly 100% accuracy.

The confusion matrix were obtained from 100 trials, with randomly selected images used in each trial. The first row of the matrix presents the results for the ResNet-18 model. The first matrix corresponds to a 1% training ratio and a 99% test ratio. The results are provided in percentages rather than absolute numbers. Given that the dataset contains 1,000 images, test matrix values can be converted into absolute numbers by multiplying them by the total test sample count. In the first matrix, where 990 images were tested, the first element of 81% indicates that 802 images were correctly classified, while the sum of the other percentage values in the same row represents the 88 misclassified images. Additionally, a value of 5% in the row suggests that

approximately 50 images were misclassified into the "Day 2" category. When the training ratio was increased to 5%, no off-diagonal elements appeared in the confusion matrix, indicating flawless classification across all three models.

The findings of this study emphasize the necessity of implementing preventive measures such as antioxidant supplementation or low-temperature storage to maintain the oxidative stability of fish oils obtained from fish waste throughout storage. Although the classification was performed based on storage day labels, the underlying premise of the image-based model is the progressive visual transformation of the fish oil due to oxidative degradation. Features learned by the ResNet architecture (e.g., color intensity, turbidity, or surface reflectance) are inherently linked to the physicochemical changes in the oil over time. Therefore, the classification results indirectly reflect the degree of oxidation rather than merely the passage of time. In other words, the visual features used to distinguish between days 0, 5, and 10 represent increasing levels of oxidative deterioration. This makes the model a surrogate quantification tool for assessing oxidation degree, particularly when integrated with chemical and sensor data.

In contrast, parameters like p-anisidine and conjugated dienes/trienes represent non-volatile oxidation products. These indicators were measured not to be directly detected by the gas sensors, but to assess the overall oxidation stage of the oil samples. The apparent correlation observed between sensor responses and these values does not imply direct detection but suggests that secondary oxidation also contributes to the formation of volatiles that can be captured by the sensors. In a previous study [50], a notable relationship was also established between increasing levels of lipid oxidation and concomitant alterations in the odor profile detected by e-nose system.

One of the limitations of the present study is that individual sensor responses were not calibrated against pure volatile standards such as hexanal or pentanal. Therefore, while sensor selectivity was inferred from the literature and sensor specifications, direct evidence of compound-specific sensitivity was not established. Future studies should incorporate calibration with known odorants to provide quantitative validation of sensor performance and enable more detailed modeling of oxidation-induced aroma profiles.

Conclusion

This study demonstrated that rainbow trout waste is a viable raw material for producing fish oil rich in EPA and DHA. However, the high polyunsaturated fatty acid content also makes the oil highly susceptible to oxidative degradation during storage. Although DHA contains six double bonds compared to five in EPA, it is not necessarily more stable. In fact, DHA is generally considered more prone to oxidative degradation due to a higher number of bis-allylic hydrogen atoms and a longer carbon chain. However, the observed degradation patterns in EPA and DHA may vary due to differences in positional distribution of double bonds, interaction with other lipids or antioxidants, and sample-specific matrix effects. Therefore, even though both are highly unsaturated, their oxidation rates may not follow a strictly linear relationship with the degree of unsaturation. A key finding is the strong correlation between classical oxidation indicators (PV and TBA) and the responses of selected gas sensors (MQ3, MQ131, MQ135, MQ138). This confirms the potential of low-cost sensor arrays, when combined with machine learning algorithms, for real-time, non-destructive monitoring of lipid oxidation. Compared to conventional methods, the sensor-based approach is faster, eco-friendly, and suitable for integration into automated quality control systems. The feasibility of implementing this system in industrial settings is enhanced by its use of open-source hardware (e.g., Arduino), which allows flexible customization, scalability, and low-cost deployment in food processing and storage environments. To further validate these findings, future studies should include control samples (e.g., solvent-extracted oil or untreated samples) and assess the performance of the sensor system under varying storage and processing conditions. In addition, integrating sensor outputs with sensory evaluation and predictive modeling could lead to the development of comprehensive quality management systems that align with consumer expectations and industrial needs.

Acknowledgements This work has been financially supported by the Scientific and Technological Research Council of Türkiye (TUBITAK), (Project ID: 223O471) and the authors also gratefully acknowledge the support provided by TUBITAK.

Author contributions Emre Yavuzer: Conceptualization; funding acquisition; supervision; Writing—review and editing; project administration. Dilek Yaprak Uslu: Data curation; investigation. Memduh Köse: Writing—review and editing. Mehmet Yetişen: Writing—original draft; investigation; formal analysis. Hamza Alaşalvar: Writing—original draft; investigation; formal analysis. Halil İbrahim Şimşek: Formal analysis.

Declarations

Conflict of interest The authors declare that they have no known competing financial interests or personal relationships that could have appeared to influence the work reported in this paper.

References

1. E. Yavuzer, F. Özogul, Y. Özogul, Aquacult. Int. **28**, 187 (2020)

2. Y. Safari, M. Karimaei, K. Sharafi, H. Arfaeinia, M. Moradi, N. Fattahi, J. Sci. Food Agric. **98**, 2915 (2018)
3. N.A. Hashim, S.K. Abdul Mudalip, S.Z. Sulaiman, S. Md, Shaarani, Mater. Today Proc. **42**, 222 (2021)
4. V.G. Alfio, C. Manzo, R. Micillo, Molecules 2021, Vol. 26, Page 1002 **26**, 1002 (2021)
5. B. Karsli, J. Food Compos. Anal. **103**, 104105 (2021)
6. T.L. Amorim, M.A. de la Fuente, M.A.L. de Oliveira, P. Gómez-Cortés, ACS Food Sci. Technol. **1**, 318 (2021)
7. P. Jayasinghe, I. Adeoti, K. Hawboldt, JAOCS J. Am. Oil Chemists' Soc. **90**, 1903 (2013)
8. E. Delgado, D.J. Valles-Rosales, N.C. Flores, D. Reyes-Jáquez, Aquac Rep. **19**, 100588 (2021)
9. P.M. Kris-Etherton, W.S. Harris, L.J. Appel, Circulation. **106**, 2747 (2002)
10. O.P. Ward, A. Singh, Process Biochem. **40**, 3627 (2005)
11. M.T. La Rovere, J.H. Christensen, Vascul Pharmacol. **71**, 1 (2015)
12. A.M. Giudetti, R. Cagnazzo, Prostaglandins Other Lipid Mediat. **99**, 57 (2012)
13. A. Jayedi, S. Soltani, A. Emadi, K. Ghods, S. Shab-Bidar, Crit. Rev. Food Sci. Nutr. **64**, 12363 (2024)
14. C. Bailly, Eur. J. Pharmacol. **931**, 175191 (2022)
15. B.N.Y. Setty, S.G. Betal, R.E. Miller, D.S. Brown, M. Meier, M. Cahill, N.B. Lerner, N. Apollonsky, M.J. Stuart, Prostaglandins Leukot. Essent. Fat. Acids. **146**, 11 (2019)
16. H. Che, M. Zhou, T. Zhang, L. Zhang, L. Ding, T. Yanagita, J. Xu, C. Xue, Y. Wang, J. Funct. Foods. **41**, 9 (2018)
17. J. Roy, Y. Mercier, L. Tonnet, C. Burel, A. Lanuque, A. Surget, L. Larroquet, G. Corraze, F. Terrier, S. Panserat, S. Skiba, Physiol. Behav. **213**, 112692 (2020)
18. L. Cao, J.Y. Si, Y. Liu, H. Sun, W. Jin, Z. Li, X.H. Zhao, R. Le Pan, Food Chem. **115**, 801 (2009)
19. Y.Z. Huang, Y. Liu, Z. Jin, Q. Cheng, M. Qian, B.W. Zhu, X.P. Dong, Compr. Rev. Food Sci. Food Saf. **20**, 3504 (2021)
20. G.C. Silvello, A.R. Alcarde, J. Agric. Food Res. **2**, 100037 (2020)
21. X. Zhan, Z. Wang, M. Yang, Z. Luo, Y. Wang, G. Li, Measurement. **158**, 107588 (2020)
22. D. Zhu, X. Ren, L. Wei, X. Cao, Y. Ge, H. Liu, J. Li, Sci. Hortic. **260**, 108879 (2020)
23. J. Wang, M. Chang, W. He, X. Lu, S. Fei, G. Lu, Sens. Actuators B Chem. **9**, 128068 (2020)
24. E. Yavuzer, Food Biosci. **41**, 100948 (2021)
25. H. Huang, X. Chen, Y. Wang, Y. Cheng, Z. Liu, Y. Hu, X. Wu, C. Wu, Z. Xiong, J. Food Sci. **89**, 9137 (2024)
26. P. Li, Z. Li, Y. Hu, Z. Niu, Z. Wang, H. Zhou, X. Sun, J. Food Sci. **89**, 5016 (2024)
27. E. Yavuzer, M. Köse, H. Uslu, J. Food Meas. Charact. **18**, 5629 (2024)
28. A. Bezama, A. Paiano, J. Hildebrandt, C. Arcidiacono, B. Bashiri, J. Cropotova, K. Kvangarsnes, O. Gavrilova, R. Vilu, Resources 2024, Vol. 13, Page 61 **13**, 61 (2024)
29. E. Ghohestani, J. Tashkhourian, B. Hemmateenejad, Food Chem. **403**, 134345 (2023)
30. A.B. Bhattacharya, M.G. Sajilata, R.S. Singhal, Food Chem. **109**, 808 (2008)
31. G. Singh, S. Maurya, M.P. de Lampasona, C. Catalan, Food Control. **17**, 745 (2006)
32. H.W. Chang, T.B. Tan, P.Y. Tan, F. Abas, O.M. Lai, Y. Wang, Y. Wang, I.A. Nehdi, C.P. Tan, Food Hydrocoll. **80**, 186 (2018)
33. K.N. ichi Ichihara, A. Shibahara, K. Yamamoto, T. Nakayama, Lipids. **31**, 535 (1996)
34. Y. Chu, J. Mei, J. Xie, Food Chem. X. **20**, 100968 (2023)
35. M.T. Golmakani, M. Moosavi-Nasab, M. Raayatpisheh, Z. Dehghani, Process Biochem. **139**, 33 (2024)
36. L. Fiori, M. Solana, P. Tosi, M. Manfrini, C. Strim, G. Guella, Food Chem. **134**, 1088 (2012)
37. S.P. Aubourg, Food Res. Int. **32**, 497 (1999)
38. P.J. Honold, M.L. Nouard, C. Jacobsen, Eur. J. Lipid Sci. Technol. **118**, 967 (2016)
39. H.H.F. Refsgaard, P.M.B. Brockhoff, B. Jensen, J. Agric. Food Chem. **48**, 3280 (2000)
40. E. Kotsoni, E. Daukšas, G.H. Aas, T. Rustad, B.K. Tiwari, J. Cropotova, Mar. Drugs 2024. **22**, 261 (2024)
41. T.T.H. Mai, Y. Choi, H. Park, J.L. Cheon, J.S. Choi, D. Park, H. Kim, Appl. Biol. Chem. **66**, 1 (2023)
42. S. Iqbal, S. Haleem, M. Akhtar, M. Zia-ul-Haq, J. Akbar, Food Res. Int. **41**, 194 (2008)
43. Y. Zhong, T. Madhujith, N. Mahfouz, F. Shahidi, Food Chem. **104**, 602 (2007)
44. S. Tavakoli, M. Naseri, E. Abedi, A. Imani, Food Sci. Nutr. **6**, 953 (2018)
45. A.E. Ghaly, D. Dave, S. Budge, M.S. Brooks, Am. J. Appl. Sci. **7**, 859 (2010)
46. Z. Noori Hashem Abad, S.H. Hosseinipour, S.M. Ojagh, Fisheries Sci. Technol. **2**, 75 (2013)
47. H.A. Al-Kahtani, H.M. Abu-Tarboush, A.S. Bajaber, M. Atia, A.A. Abou-Arab, M.A. El-Mojaddidi, J. Food Sci. **61**, 729 (1996)
48. F. Sabzipour, M. Naseri, S. Babaei, A. Imani, Food Sci. Nutr. **7**, 3093 (2019)
49. C. Karungi, Y.B. Byaruhanga, J.H. Muyonga, Food Chem. **85**, 13 (2004)
50. G.M. Dong, R.Y. Wang, F.W. Yin, D.Y. Li, L. Qin, D.Y. Zhou, Food Chem. **485**, 144475 (2025)

Publisher's Note Springer Nature remains neutral with regard to jurisdictional claims in published maps and institutional affiliations.

Springer Nature or its licensor (e.g. a society or other partner) holds exclusive rights to this article under a publishing agreement with the author(s) or other rightsholder(s); author self-archiving of the accepted manuscript version of this article is solely governed by the terms of such publishing agreement and applicable law.